Advances in Colloid and Interface Science
94 (2001) 167–196

ADVANCES IN COLLOID AND INTERFACE SCIENCE

www.elsevier.com/locate/cis

The glass transition in thin polymer films

James A. Forrest[a,*], Kari Dalnoki-Veress[b,1]

[a] *Department of Physics and Guelph–Waterloo Physics Institute, University of Waterloo, Waterloo, Ontario, Canada N2L 3G1*
[b] *Department of Physics and Astronomy, University of Sheffield, S3 7RH Sheffield, UK*

Received 29 May 2000; accepted 18 August 2000

Abstract

In this article, we present a detailed account of important recent developments in the rapidly evolving area of glass transitions in thin polymer films. We review the case of polymer films supported by substrates, and show that a definite experimental consensus exists. We consider recent results from experimental studies of free-standing films of polystyrene. These studies have provided a thorough quantification of the behavior of glass transition anomalies in free-standing polymer films, and have served to motivate recent attempts at theoretical descriptions. We introduce and examine models, which have been proposed to explain the experimental observations and discuss the significance of these models.

Keywords: Glass transition; Thin polymer films; Dynamics in confinement

Contents

* Corresponding author.
E-mail address: jforrest@uwaterloo.ca (J.A. Forrest).
[1] Present address: McMaster University, Hamilton, Ontario, Canada L8S 4M1

0001-8686/01/$ - see front matter
PII: S0001-8686(01)00060-4

1. Introduction

Glass forming substances are ubiquitous materials. Organic liquids, polymers, and even metals can all undergo a glass transition and form a glassy rather than crystalline solid. Despite the obvious technological importance of glass forming materials, it has to be noted that the glass transition itself, though well characterized, is generally not well understood. The lack of understanding is reflected in the fact that there are no theories which even claim to offer a description of all aspects of the dynamics of glass forming materials. The well-known free volume model of Cohen and Turnbull [1] is an intuitive and appealing picture, but the approach is phenomenological in nature and the free volume is not rigorously defined. The mode coupling theory of Sjögren and Götze [2] is successful at describing the dynamics of many glass formers at high temperatures, but fails to describe the dynamics at temperatures near the calorimetric glass transition. Thermodynamic theories of the glass transition also exist [3], but except for a few instances [4], do not readily lead to a description of the dynamics.

One concept, which is often used in the description of glass transition dynamics, is the idea of co-operative motion. The basic idea behind the approach, first introduced empirically by Adam and Gibbs [5], is that as the temperature in a glass forming material is brought near the glass transition temperature, individual particle motion is frozen out. The result is that the only structural rearrangements, which may occur must involve the collective movement of many particles, and the length scale for co-operative dynamics must be temperature-dependent, increasing as the temperature is lowered. In a more rigorous approach, Edwards and Vilgis [6] developed an exactly solvable model system for glass transition dynamics and were able to show that co-operative motion alone was enough to give rise to a Vogel–Fulcher temperature dependence of relaxation times on temperature. Recent computer simulations [7,8] have revealed the existence of co-operative motion where particle motion occurs in string-like clusters. The dimension of such clusters is fractal, but ~ 1, and the number of units in a cluster was found to increase with decreasing temperature. Computer simulations have also revealed a strong dy-

namic heterogeneity in glass forming materials. The co-operative motion is found to exist only within mobile clusters, and the length scale for this dynamic heterogeneity is expected to be closely related to that of co-operative motion and is found to have qualitatively the same temperature dependence. While most simulations have involved simple particles interacting through a Lennard–Jones potential, similar results have been found for polymers. A growing length scale for dynamics has been observed in molecular dynamics simulations of a polymer melt [9], as has a clustering of mobile monomer units [10]. From the evidence provided by theory and simulation it is reasonable to define a length scale $\xi(T)$, for the dynamics of glass forming materials.

Our picture of a glass forming liquid near T_g, is one which is on average homogeneous, but instantaneously heterogeneous, and consists of some regions which are more liquid-like and others which are more solid-like. These regions are not necessarily strongly correlated to density fluctuations. Since these regions are structurally indistinguishable, and differ only in their dynamics, there is no hope to use scattering methods to determine the length scale $\xi(T)$. Instead the only way to ascertain the existence of such a length scale is through the use of *finite size effects.* The central idea behind finite size effects is easily described. The sample is confined to a size D. At high enough temperatures $\xi(T) \ll D$, the dynamics of the confined system will be the same as the bulk system. As the temperature is lowered, $\xi(T)$ increases and eventually the condition $\xi(T) \sim D$, will be reached. When $\xi(T) \sim D$, the confined system will exhibit anomalous dynamics compared to the corresponding bulk system. The way the dynamics of the confined system will be affected depends strongly on the boundary conditions of the system. From the concept of co-operative motion, it is clear that if the molecules on the boundary are held fixed (strongly attractive interaction in an experiment), then the confined system will exhibit much slower dynamics than the bulk system or may even be completely arrested. Alternatively, if the molecules on the boundary have a high degree of freedom (such as in the experimental case of a free surface), then the dynamics of the confined system will be faster than that of the bulk system.

The first comprehensive study of glass forming materials in highly confined geometries were the calorimetric studies of Jackson and McKenna [11]. These studies involved organic glass forming liquids confined to the pores of Vycor glass. The T_g values for the confined systems were less than that of the bulk with a maximum effect for *o*-terphenyl confined to 40 Å pores where the T_g value was reduced 18 K below the bulk value. More recent studies of glass formers confined in pore glass have involved dielectric spectroscopy [12]. These studies have revealed faster dynamics in confined systems and have suggested a length scale for glass transition dynamics of 30–70 Å. A complication, which has been noted for using pore glass as the confining medium is the influence of the interfacial interaction. It has been found that the observed dynamics depend strongly on the treatment of the pore surface [13]. Furthermore, once treated, it is difficult to quantify the interfacial properties. A second disadvantage of such studies is that the confinement dimension, which may be probed, is limited by that of available pore glass while the pore size distribution can be broad.

An attractive sample choice for studies of finite size effects is that of thin polymer films. Foremost among the advantages of this sample geometry is that the confining dimension, the film thickness, can be continuously varied over many orders of magnitude from nanometers to micrometers. Furthermore, there are a large number of polymers which will readily vitrify rather than crystallize, and this, combined with many substrate materials and treatments, allows a range of interfacial interactions to be investigated. Utilizing polymer film samples also allows for the preparation and study of free-standing films. We shall show later that the ability to study free-standing films has provided many advances in the study of finite size effects in polymer film samples. The interfacial interaction between a polymer and substrate is also readily quantified by the use of contact angle measurements. However, the use of polymeric materials introduces complications which do not exist when studying other glass formers. Polymer molecules are extended objects with a characteristic size, the r.m.s. end-to-end distance $R_{EE} \propto N^{1/2}$, where N is the number of monomer units. This inherent length scale introduces the possibility of *chain confinement effects* as the film thickness h becomes smaller than the unperturbed molecular size. Such effects may be very difficult to distinguish as they can introduce anomalies in the dynamics without necessarily causing any changes in the structural properties. One way in which it may be possible to identify chain confinement effects is that the magnitude of such an effect, for constant film thickness, should depend on the molecular size. While the existence of chain confinement effects may obscure observation of finite size effects, they are interesting in their own right as they serve as a probe of fundamental aspects of perturbations of polymer dynamics.

2. Measuring the glass transition in thin films

As the temperature of a glass-forming material is lowered, the relaxation times become very large. A result of this is that certain types of motion will be frozen out on the time scale of a particular experiment, and they no longer contribute to such quantitities as the thermal expansion or heat capacity. Since the relaxation times vary strongly with temperature, there is an apparent discontinuity in these thermodynamic quantities. Thus, the kinetic glass transition appears experimentally to be quite similar to a second order thermodynamic phase transition. In bulk materials, T_g is either defined in terms of these near discontinuities, or alternatively, when certain relaxation times are equal to a predefined value (usually 100 s). All of these 'definitions' of the glass transition lead to approximately the same measured T_g value. Since the measured T_g value depends on the thermal treatment of the sample, including the heating and/or cooling rate during the measurements, it is important to know the measurement conditions when making comparisons between different experiments.

For the case of thin polymer films, the most common measurement techniques are those that probe, directly or indirectly, the thermal expansion of the sample [14]. Ellipsometry is the most common technique to measure T_g in supported

polymer films, and has even recently been applied to free-standing films. Ellipsometry measures the ellipticity induced upon interaction with (either reflection from or transmission through) a sample. For a simple isotropic polymer film, the measured quantities can be related in a straightforward manner to the refractive index (n) and thickness (h) [15] of the thin film. Furthermore, small changes in thickness and refractive index typical of most of the ellipsometry experiments, can be shown to be linearly related to small changes in the ellipsometric measurables. Since both these quantities vary with the density of the sample, they necessarily exhibit a 'kink' at the glass transition temperature T_g. The inversion of raw ellipsometric data to obtain thickness and refractive index as a function of temperature has been carried out for the case of both supported [16,17] and free-standing [18] films. For both types of samples, the T_g obtained from the raw ellipsometric data was the same as that obtained from analysis of the thickness vs. temperature data. In practice, the relation between the physical quantities h and n, and the ellipsometric variables P and A, means that the inversion to h and n is rarely carried out. Ellipsometry has been shown to be capable of measuring T_g values in supported polymer films as thin as 50 Å and free-standing films as thin as 200 Å.

The common method of determination of T_g is by selecting two linear regions of the data and finding the intersection point between the extrapolated lines. While this method is generally satisfactory, it relies on an initial estimate of T_g, which necessarily affects the results. To avoid this bias, an alternative method has recently been employed [18]. In the glass transition region, the thermal expansion coefficient varies from that of the glass to that of the melt over a very small temperature range. This 'near discontinuity' at the transition is well described by a tanh-profile. By integrating this 'tanh' profile one can derive the following expression for the film thickness, which is also applicable for measurement of any quantity that varies linearly in the melt and glass region with temperature:

$$h(T) = w\left(\frac{M-G}{2}\right)\ln\left[\cosh\left(\frac{T-T_g}{w}\right)\right] + (T-T_g)\left(\frac{M+G}{2}\right) + c. \qquad (1)$$

Here c is the value of the film thickness at $T = T_g$, w is the width of the transition between the melt and the glass, and M and G are the dh/dT slope values for the melt and glass, respectively. A value of T_g may be obtained by fitting $h(T)$ to Eq. (1). The standard determination of T_g has 4 explicit parameters for the two linear regions, and additional 2 implicit parameters in the *choice* made for the beginning and end of the transition region. In addition to having less free parameters, Eq. (1) avoids the ambiguity of the more standard method of determining T_g.

A second technique, which has been successfully used to measure T_g in thin supported films, is that of X-ray reflectivity. This technique is also able to provide a sufficiently accurate measure of film thickness to allow measurements of T_g. A limiting factor in the utilization of reflectivity techniques vs. ellipsometric ones is the rate at which data can be acquired. In a typical ellipsometric experiment, the

data acquisition rate is sufficient that many data points can be required per degree while ramping the temperature at rates as high as 10 K/min. In contrast, reflectivity techniques require the sample to be held at constant temperature for many minutes for each datapoint. Recently, a number of other techniques have been used to measure T_g in thin films. Such techniques include positron annihilation lifetime spectroscopy [19] (a technique also used in bulk polymers), optical waveguide spectroscopy [20], and capacitance measurements [21,22].

For the case of free-standing films, there is a much more limited range of techniques, which have been utilized to measure the T_g value. Foremost among these techniques is that of Brillouin light scattering (BLS) [23–25]. By measuring the frequency shift of light, which is scattered from thermally excited film guided acoustic phonons, a sensitive probe of the material density is provided [26,27]. BLS has been used successfully to measure T_g for free-standing polymer films with thicknesses as small as 200 Å. One unfortunate aspect of the BLS technique is that determination of a single T_g value can take as long as 20 h. Recently, transmission ellipsometry has been used to measure T_g in free-standing films [18]. Ellipsometry provides a much more rapid measurement, but suffers from a higher sensitivity to sample defects such as wrinkles, than does BLS.

3. The glass transition in supported polymer films

3.1. Measurements of the glass transition in supported films

The first systematic investigation of T_g values in thin polymer films was performed by Keddie, Jones and Cory [16], and involved ellipsometric measurements of T_g in films of polystyrene (PS) supported on hydrogen passivated Si(111) wafers. The film thickness, h, was varied from $\simeq$ 3000 Å down to $\simeq$ 100 Å. This study revealed the remarkable observation that the T_g values for films with $h \lesssim 400$ Å was reduced below the bulk value. This reduction in T_g was found to increase as the film thickness was lowered. The lowest measured T_g value was 25 K less than the bulk value and was observed for a film thickness of 100 Å. Films composed of PS with M_w values ranging from 120×10^3 to 2900×10^3 (R_{EE} from $\simeq$ 200 to $\simeq$ 1000 Å) were studied in order to investigate the importance of polymer chain confinement. For all samples considered, the measured T_g values were independent of M_w and the data were collectively described by the empirical relation

$$T_g = T_g^{\text{bulk}}\left[1 - \left(\frac{a}{h}\right)^{\delta}\right] \tag{2}$$

where T_g^{bulk} is the value of T_g for bulk PS. The best fit to the measured T_g values was provided by $a = 32$ Å and $\delta = 1.8$. This effect was suggested as being dominated by the existence of a liquid-like layer near the free surface with a characteristic size which increased as the temperature was raised and diverging at T_g. The intuitive idea of a surface layer with higher mobility is still incorporated

into more recent attempts at modeling. However, the idea of a length scale of mobility which increases with temperature is in contrast with the temperature dependence predicted (and observed in simulations) for the length scale of co-operative motion. There is also no evidence for a length scale, which diverges with increasing temperature from other experiments or simulations. Kim et al. [28] have recently proposed an alternative parameterization of the data which allows T_g data for thin films of many different polymers to be described with only a single material-dependent fit parameter.

In order to gain an understanding of the glass transition in more general terms, it is important that finite size effects in polymer films are not restricted to a single polymer material and, instead, exhibit some degree of universality. Recent measurements have confirmed that the T_g anomalies are not peculiar to the polymer PS. Using the technique of optical waveguide spectroscopy, Prucker et al. [20] have shown that for PMMA films supported on hydrophobic glass substrates (treated with HMDS), the measured T_g values decrease with decreasing film thickness. In complete analogy to the data for PS, the T_g values for the PMMA thin films were also found to be described by Eq. (2). For PMMA, the parameters were $a = 3.5$ Å and $\delta = 0.8$ [20], which were different from those for PS. The ability of the same functional form to describe the data for the two polymers is intriguing, but since Eq. (2) is purely empirical, it is not possible to ascribe physical meaning to either of the parameters. Finally, it is worth noting that very similar behavior in T_g vs. h has also been observed for thin polycarbonate films [17] as well as films of poly(α-methyl styrene) and polysufone [28]

Since the initial investigations of Keddie et al., there have been many other studies for PS on a variety of different substrates, and employing a number of experimental techniques. Researchers using ellipsometry [24], X-ray reflectivity [29], positron annihilation [19], and dielectric [22] techniques have all reached the same conclusion — the T_g value of thin PS films is reduced below the bulk value, and this effect becomes more pronounced for films with smaller values of film thickness. The overwhelming consensus between the conclusions from these different studies is best demonstrated by Fig. 1, which shows all measured T_g values presented in the literature for thin PS films supported on substrates. For reasons of clarity, we have not distinguished the results of different studies. A similar plot, which does differentiate the different groups, but does not include the recent T_g data of reference [22], can be found in reference [30].

While there is some scatter in the quantitative values, the qualitative trend mentioned above is completely obvious. This agreement between a variety of techniques also serves to validate each of the techniques used. Despite the large number of experimental studies of the T_g value in thin supported films, very few ideas have been put forth regarding the origin of the effect. The most likely reason for this is the scatter between the results from the different studies in Fig. 1, which suggests that the details of the interaction between the polymer and the substrate are important to get quantitative agreement between different studies. This complication is removed in the studies of free-standing films, and it was exactly this fact that first motivated measurements of T_g in free-standing films.

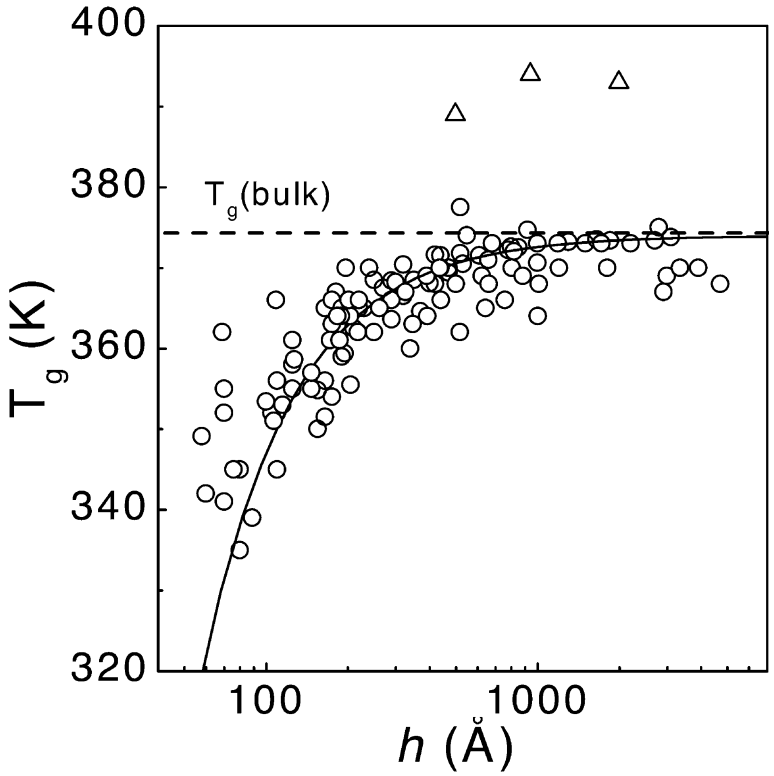

Fig. 1. Compilation of all measured T_g values for supported PS films. Measured values are from references [16,19,21,22,24,29,35].

The importance of the polymer substrate interaction was recognized early and this has resulted in a number of studies aimed at directly studying this effect. One such study was an extension of the ellipsometric studies of Keddie et al. to ultrathin films, which were physically grafted to the substrate [31]. For such thin films, it may be argued that the polymer substrate interaction will dominate the behavior, and it was observed that for sufficiently thin films the trend of T_g decreasing with h is actually reversed, and for films with 50 Å $< h <$ 100 Å, the measured T_g values increase with decreasing film thickness. A quantitative explanation for this observation has recently been suggested [25]. An alternative to studying ultrathin films to focus on the effect of the polymer–substrate interaction is to study systems where one expects a much stronger attractive interaction. One example of this is the study by van Zanten et al. for poly-2-vinylpyridine on oxide-coated Si substrates [32]. In this system the measured T_g value was observed to increase above the bulk T_g, with a maximum increase of 50 K for a 77-Å film.

Perhaps the most extensive body of data concerning the influence of the polymer substrate interaction on the measured T_g value is for polymethyl methacrylate

(PMMA). Keddie et al. showed that the nature of this interaction could qualitatively change the thickness dependence of the T_g value [33]. For PMMA films on Au-coated glass substrates, the measured T_g value was found to decrease with decreasing film thickness. For the same polymer on oxide-coated Si, the T_g value was found to increase above the bulk T_g for sufficiently thin films. Later studies by Grohens et al. [34] using PMMA molecules with different tacticity were able to show a direct correlation between the density of polymer substrate interaction with the measured T_g value. While the T_g value of many polymers has been shown to be sensitive to the substrate used, it does not appear to be sensitive to the method of preparing the thin film. For the case of PS, Keddie et al. showed that spincast films behaved quantitatively similar to grafted ones. For PMMA, Prucker et al. observed similar T_g reductions for films, which were spincast, grafted, or prepared using the Langmuir–Blodgett technique [20].

3.2. Resolving controversy in thin film T_g studies

The discussion above demonstrates the importance of the strength of interaction between the polymer and substrates on measured T_g values. In contrast, Fig. 1 clearly shows that for the case of PS, this interaction does not appear to dominate the behavior. This contradiction is most clearly illustrated in the widely discussed *apparent* discrepancy between the studies of Keddie, Jones and Cory [16], and a similar study on the same system using X-ray reflectivity [35]. The reflectivity study claimed that the T_g value for PS films on hydrogen-passivated Si substrates was increased to a value at least 40 K greater than their measured bulk T_g for film thickness $h \lesssim 400$ Å. The contradiction with the results of reference [16] was suggested to be due to a strong sensitivity to slight differences in the substrate properties. While this claim was not supported by any *actual measured* T_g values, which increased for decreasing film thicknesses, the study continues to be widely cited as an important example of the extreme sensitivity of the T_g value to the substrate properties. As shown in Fig. 1, there is a large body of experimental evidence which demonstrates that for the case of PS films the T_g values are only weakly sensitive to the properties of the substrate. Given now that reference [35] stands out in contrast to many other studies, it is prudent to consider it in more detail.

Fig. 2 reproduces the X-ray reflectivity data of reference [35]. For the three thickest films, a T_g can be determined from the data by the kink in the thickness vs. temperature data. For the thinnest film shown in Fig. 2, (and apparently for all films with $h \lesssim 437$ Å) no break in the thickness vs. temperature data can be distinguished and the slope of the data is consistent with a glassy value of the thermal expansion coefficient. This led to the inference that for films with $h \lesssim 437$ Å the T_g value had *increased* to a value greater than the maximum temperature considered — in this case 430 K. The implication was that the T_g value increased from $\simeq 390$ K for $h = 497$ Å to a value greater than 430 K for $h \lesssim 437$ Å (in these measurements bulk $T_g^{\text{bulk}} = 390$ K, i.e. ~ 20 K greater than the typical value for PS). While it is *possible* that the T_g value increases from the bulk value to one

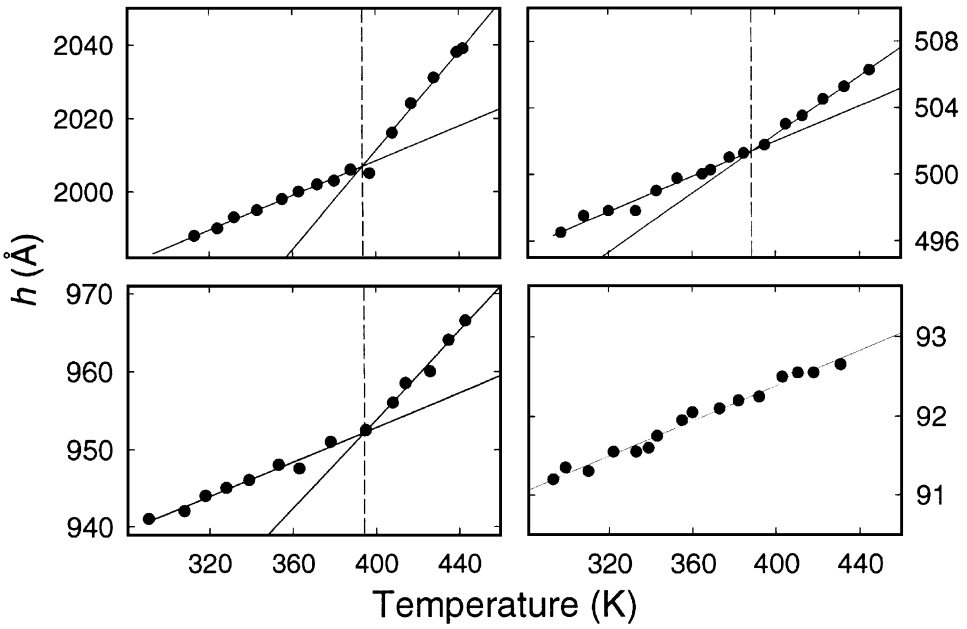

Fig. 2. Film thickness vs. temperature data from reference [35]. The solid lines are the linear fits to the glass and melt temperature regions, which were used to measured the T_g values.

at least 40 K higher in such a small range of thickness that intermediate T_g values cannot be observed, it does not seem likely. This is especially true given the consensus of all of the measurements shown in Fig. 1.

An alternative explanation for the data presented in reference [35] and reproduced in Fig. 2 has also been suggested in references [24,30]. The explanation allows all data to be explained in a simple unifying framework with no resulting contradictions. Furthermore, this approach, using the data of reference [35] highlights another anomalous property of thin PS films. An analysis of the slopes of the thickness vs. temperature data in Fig. 2 reveals that while the thermal expansivity $\left(\frac{1}{h}\frac{\mathrm{d}h}{\mathrm{d}T}\right)$ in the glassy state is the same for all film thicknesses, the thermal expansivity of the melt state varies with film thickness; decreasing as the film thickness is lowered. The most important consequence of this fact is that the contrast of the transition; the ratio of the melt expansivity to that of the glass is also a decreasing function of film thickness. As the contrast of the transition decreases, it becomes more and more difficult to identify the transition. For a contrast of 1 it is, by definition, not possible to identify a transition at all. In practice, any data will exhibit some scatter, and identification of the glass transition becomes impossible for a contrast value somewhat greater than unity. The decrease in contrast for decreasing film thickness is evident from Fig. 2, and is further quantified in Fig. 3.

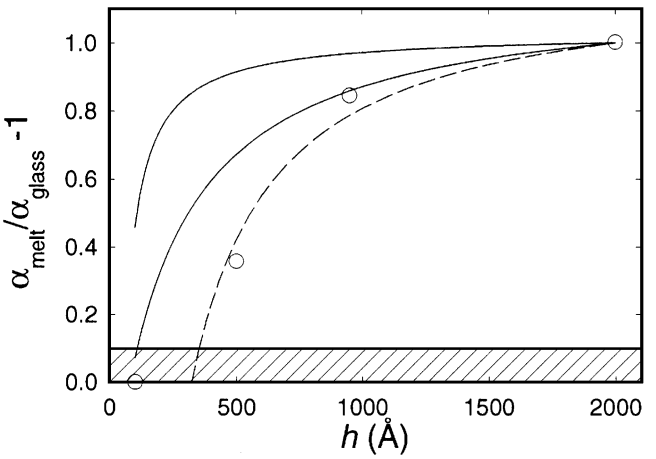

Fig. 3. Normalized glass transition contrast for thin PS film. The solid curves are the $1/h$ fits from references [17] (upper curve) and [26] (lower curve), and the data points are obtained from Fig. 2. The dashed curve is a $1/h$ fit to the contrast values found from Fig. 2.

The plot in Fig. 3 explicitly shows the film thickness dependence of the thermal expansivity. The data points are measured values of the transition contrast, normalized so that different studies may be compared. In this plot a value of zero corresponds to no transition contrast (i.e. the glass and melt expansivities are the same), and the shaded region represents the range of contrast for which it is generally not possible to identify the 'kink' needed to measure T_g. Also shown on this graph is the film thickness dependence of the contrast for two additional studies [16,19], which both showed T_g values decreased below the bulk value. These two solid curves are fits to a $1/$h functional form, which was used in both studies to parameterize the results, and can be shown to be consistent with a multilayer model for the polymer film dynamics incorporating a melt-like layer at the free surface. It is evident that all of these studies show the same qualitative decrease in the contrast of the transition. A more detailed comparison reveals that there are systematic deviations between the studies, which will lead to different limiting values of the film thickness where a T_g can be observed. The dashed lines in this figure correspond to a fit of the symbols to a $1/$h film thickness dependence. This representation shows that while the data of reference [35] does not support a T_g value, which increases as the film thickness is lowered, it certainly *does* support a decreasing contrast of the glass transition. In fact the extrapolation provided by the dashed line fit demonstrates that the reflectivity studies should *not* be able to determine a T_g for films with $h \lesssim 400$ Å. The alternative explanation for the data in reference [35] is simply that the glass transition still occurs in the experimental temperature window, but with too low a contrast to be identified. We reiterate that this decrease in contrast is observed in *all* studies of T_g in thin films and has been studied explicitly in references [16,19], and that this simple explanation, supported by other experimental studies, resolves the controversy associated with this work.

While many studies have reported this decrease in the contrast of the transition, there is a remaining discrepancy in which expansivity is dependent on film thickness. The data in reference [35] clearly shows that it is the expansivity in the melt which varies with film thickness, and this conclusion is supported by the PALS study of reference [19] as well as by studies of free-standing films [36]. The ellipsometric study of reference [16] suggests instead that it is the expansivity of the glass, which varies with film thickness. This issue is currently unresolved, and more detailed study of thermal expansion in thin films is certainly warranted. Finally, we note that in BLS studies of the contrast of the glass transition in free-standing films, a much more complicated behavior was observed with a contrast which did not decrease monotonically in the same way that Fig. 3 demonstrates for supported polymer films [36].

A second area of controversy in the glass transition of thin films involves attempts to measure the dynamics more directly. A straightforward way to probe dynamics in thin films is to look at the diffusion of entire chains. Such studies have been performed and have found the somewhat surprising result that the diffusion of PS chains both in the plane of the film [37] as well as normal to the film plane [38], are reduced for thin films compared to thick films or bulk samples. The reductions in chain diffusion occur for film thickness $h \lesssim 1000$ Å. The observation of slower chain motion seems to disagree with the idea of lower T_g values in thin films, which would suggest an enhanced mobility. It should be noted, however, that the changes in diffusion are observed for substantially thicker films than those exhibiting T_g reductions. Inferences about T_g from the dynamics of entire chains must be made with care as higher segmental mobility is obviously a *necessary* condition for enhanced chain mobility, but it may not be a *sufficient* condition. For example, pinning a small fraction of a polymer chain can lead to a case where the chain will not be able to diffuse (leading to a vanishing diffusion constant) even for very high segmental mobility. This example suggests that a series of measurements at a single temperature and decreasing film thicknesses does not provide a quantity which can be compared in a straightforward manner with measured T_g values. This may be stated more quantitatively if we recall that the chain diffusion will be of a Vogel–Fulcher form with $D(T) \sim D_0 \exp[-B/(T_0 - T)]$, where $T_0 \sim (T_g - 50\ \mathrm{K})$. We have already suggested that the observed changes in the thermal expansivity of the thin film melt, which are observed for films with $h \lesssim 1000$ Å, may be caused by certain types of motion not contributing to the thermal expansivity. It is obvious that the freezing out of any type of motion should result in slower chain diffusion. The manifestation of this effect in chain diffusion studies will be a film thickness dependence of D_0. This in turn leads to the observed slower diffusion *independent* of any changes in the T_g value of the film. We stress that in order to use chain diffusion studies to compare to the T_g value, it is the *temperature dependence* of the diffusion constant, which must be measured. Such measurements have not yet been performed. Finally, we note that measurements in both free-standing and supported films have been performed to look at the segmental dynamics, which *are* expected to couple directly with the T_g. In this case, complete agreement has been

found between measured segmental dynamics and measured T_g values [21,22,39] as is discussed in more detail below.

3.3. Other probes of dynamics in thin polymer films

Measurements of the glass transition are an indirect probe of the dynamics in thin polymer films, and provide a single value to describe the entire temperature-dependent dynamics of the system being measured. In addition to the measurements of whole chain diffusion discussed above, there have been a number of recent studies, which focused on measuring the dynamics in thin polymer films. The suggestion that reduced T_g values result from enhanced dynamics at the polymer free surface, has prompted studies aimed at directly measuring the relaxation properties of the polymer surface.

The first direct measurements of relaxation dynamics in thin polymer films were made by Hall et al. using second harmonic generation [40] to study probe-doped polymers. These studies revealed that for films with decreasing film thickness, the relaxation functions became broader, but the average relaxation time remained the same. These results were noted to be consistent with the small changes in T_g observed for thin films of the polymer, poly(methyl methacrylate). More direct comparisons with the data in Fig. 1 can be made by considering studies on relaxation in thin films of PS. Quartz crystal microbalance measurements of the adhesion of small particles to thin PS films, have been used to obtain a signature of relaxation [39]. The film thickness of this relaxation signature was found to agree quantitatively with the data in Fig. 1. Recent studies by Schwab et al. [41] have measured the relaxation of birefringence induced by rubbing thin films of PS. These studies revealed that for films less than ~ 250 Å, the relaxation was much faster than that for thicker films and corresponded to a decrease in the T_g value of 15–20 K. Dielectric spectroscopy has also been employed to measure the relaxation function of thin PS films on Al-coated substrates [21,22]. The relaxation functions obtained agree quantitatively with the measured T_g values, but this agreement appears to be a result of a substantial broadening of the relaxation function rather than a simple shift to lower temperature. Further studies to directly probe relaxation functions in thin films should help to clarify these initially intriguing observations.

Measurements of relaxation of the polymer surface offers tremendous promise as a direct probe of the proposed enhanced surface mobility used to explain T_g reductions in thin films. A variety of experimental techniques have been applied to this problem, but a clear experimental consensus has not yet emerged. Positron annihilation techniques have been used to probe the near surface region of PS films and has led to conclusions of both enhanced [42] as well as bulk-like [43] surface dynamics. NEXAFS has been used to investigate the surface relaxation of rubbed films of PS [44]. The relaxation of the dichroism induced by the rubbing procedure was monitored and not seen for temperatures less than the bulk value of T_g. Scanning force microscopy has also been used to probe the surface properties of polymer films through the measurements of friction forces [45]. These studies

have also suggested an enhanced mobility at the polymer free surface for a number of different polymers including PS.

4. The glass transition in free-standing films

The controversy concerning the effect of the substrate in thin film T_g studies prompted studies of free-standing films. The first measurements of the T_g value in free-standing films were the BLS studies of PS films with thickness h between 200 and 2000 Å [23]. The results of this study were remarkable in several aspects. The measured T_g values in the free-standing films exhibited reductions below the bulk value, which were much greater in magnitude than those reported for supported films; with a 200-Å film having a T_g value reduced by 70 K below the bulk value. For comparison, a supported film of the same thickness exhibits a T_g reduction of only 10 K. Consistent with this larger magnitude of T_g anomalies, was the fact that T_g reductions were observed for much larger values of the film thickness; up to $\sim$ 700 Å. Finally, the film thickness dependence of the T_g values in free-standing films was found to be qualitatively different from Eq. (2). The reduced T_g values were accurately described as a linear function of film thickness. An extension of the BLS studies to a second value of M_w, revealed a strong M_w dependence of the T_g value [24], in contrast to the observations for supported films. The strong M_w dependence observed in these studies revealed the importance of *chain confinement effects* for high M_w, free-standing films. These studies emphasized the importance of a detailed study of the M_w dependence of the T_g in free-standing PS films. This is necessary to characterize in more detail, the M_w dependence, that has been observed; and also to search for any finite size effects.

The challenge for more detailed studies of T_g in free-standing polymer films has been met by two different studies, each focusing on a different M_w regime. BLS studies have been used to measure the film thickness dependence of PS films with $120 \times 10^3 < M_w < 2240 \times 10^3$ in order to explore the low M_w region [36]. This study is joined with transmission ellipsometry studies where the film thickness dependence of T_g values was studied for PS with $575 \times 10^3 \leq M_w \leq 9100 \times 10^3$ [18]. The data from both of these separate studies are shown collectively in Fig. 4, which is the free-standing film analog to Fig. 1.

Comparing Fig. 4 with Fig. 1, we notice the free-standing films exhibit a much richer behavior than their supported counterparts. Most notably, the effects on T_g are much larger than those for supported films. For values of M_w in the entire range, T_g reductions as large as 70 K are observed. More importantly, we notice a complicated M_w dependence for free-standing films, which did not exist for supported films. As was first noted in reference [36], the data seem to naturally divide into two distinct regimes of M_w. For a value of $M_w \leq 378 \times 10^3$, the film thickness dependent T_g values do not appear to exhibit any discernable M_w dependence. In addition, the dependence of T_g on h is not linear. For $M_w \geq 575 \times 10^3$, the T_g values are a linear function of film thickness with a threshold and slope, which are dependent on M_w though this dependence *appears* to saturate for

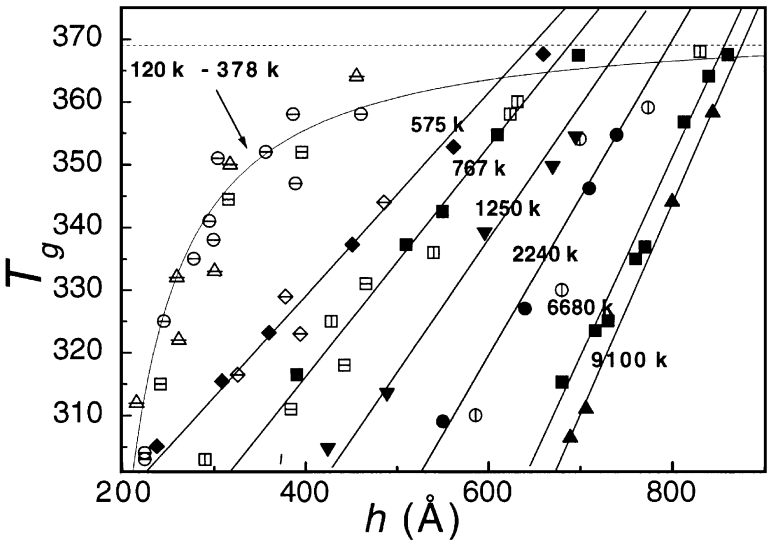

Fig. 4. Measured T_g values for free-standing polymer films. The solid symbols are obtained with ellipsometry and taken from reference [18]. The hollow symbols are obtained using BLS, with a vertical bar indicating the data from reference [24] and a horizontal bar indicating data from reference [36].

very large values of M_w. For the purposes of further discussion, we will use the suggestion provided by the data and divide the discussion into these two regimes of M_w. We note that there are no datasets exhibiting intermediate behavior.

4.1. T_g for free-standing films with $M_w \geq 575 \times 10^3$

As first noted in reference [24], the data for high M_w displays some extraordinary characteristics. For any particular value of M_w, the measured T_g values appear to be a linear function of the film thickness. For film thicknesses down to a certain threshold value h_0, the $T_g = T_g^{\text{bulk}}$, and for $h < h_0$, the $T_g < T_g^{\text{bulk}}$. The M_w dependence evident from Fig. 4 certainly shows that confinement of the polymer chains is an important factor in the T_g reductions, but the behavior is more complicated than one might at first expect. The most straight-forward explanation would be that the T_g value shows anomalies from the bulk value for $h < R_{EE}$, and thus, we would expect that h_0/R_{EE} would be constant. We might also expect the slope of $T_g(h)$ to vary in the same way so that normalizing the film thickness by plotting h/R_{EE} instead of simply h, we could collapse the data onto a single line. Unfortunately, such a simple scaling relation has been shown to be insufficient to describe the data [18]. A recent study focused on the quantification of the M_w dependence in the hope that the mechanisms responsible for T_g reductions may be understood from the scaling dependence of T_g on h and M_w [18,46]. The experimental details of this study are described by Dalnoki-Veress et al. [18] and here, we only present a brief overview. In these studies, transmission ellipsometry on

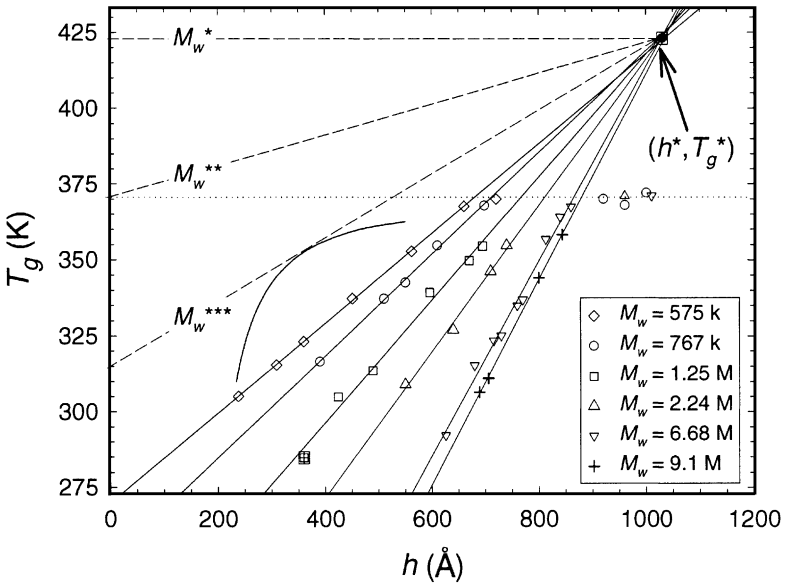

Fig. 5. Plot of T_g vs. h for the high-M_w regime ($575 \times 10^3 \leq M_w \leq 9.1 \times 10^6$). The straight solid lines are the best fit lines to the reduced T_g data and intersect at a common point (h^*, T_g^*). The solid curve represents the average reduced T_g values for the low-M_w regime. See the text for a discussion of the dashed lines labeled M_w^*, M_w^{**} and M_w^{***}.

free-standing films as a function of temperature, provided a relatively quick and straight-forward measure of T_g, making the characterization of six molecular weights ranging from 575×10^3 to 9100×10^3 possible.

The data for the high M_w study are shown in Fig. 5. One of the most striking aspects of the data is that the transition from the normal bulk glass transition to reduced T_g values as the thickness is decreased, appears to be very sharp. Despite considerable effort to measure in the transition region, no deviation from two linear regions could be observed (i.e. no curvature near T_g^{bulk}). The sudden nature of this transition is consistent with the existence of an alternative mechanism for mobility, which is distinct from that of the bulk, but becomes more important in thin films. The mechanism responsible for glass transition in bulk materials obviously results in $T_g = T_g^{\text{bulk}}$ (indicated by the dotted line in Fig. 5). As the film thickness is decreased, deviations from bulk behavior will be observed when the thin film mechanism becomes a more efficient mechanism for mobility than the bulk mechanism. This competition between two distinct mechanisms as a consistent interpretation of the data was first discussed by de Gennes [47] and later in [46], and would be expected to result in the sharp transition observed in the data.

Examination of Fig. 5 reveals that the slope α of the reduced T_g data as well as the intersection h_0 with the bulk line at T_g^{bulk} both increase monotonically with increasing M_w. A surprising aspect of the data is revealed by extending the plot to

higher T_g and h; all the best fit lines to the reduced T_g data intersect at a single point (h^*, T_g^*). This is perhaps the most powerful suggestion of the data, and clearly, regardless of the mechanism responsible for the anomalous reductions in T_g, determining the physical significance of the point (h^*, T_g^*) is crucial to developing an understanding of this mechanism. The intersection of these lines necessarily means that $(T_g - T_g^*) \propto (h - h^*)$ and we write

$$(T_g - T_g^*) = \alpha(M_w)(h - h^*), \tag{3}$$

where all the M_w dependence is now in the slope parameter $\alpha(M_w)$. The intersection of the best-fit lines to the reduced T_g data is given by $(h^*, T_g^*) = (103 \pm 1$ nm, 423 ± 2 K). The α–β splitting (the temperature at which the α-relaxation mode, associated with segmental mobility, and the β-relaxation, associated with side group relaxations, become distinct from each other) occurs at a temperature of $T_{\alpha\beta} \sim 423$ K. Though possibly a coincidence, the fact that $T_{\alpha\beta} \sim T_g^*$ introduces the possibility that the mechanism for mobility resulting in reduced T_g values in thin films, *may* be related to the motion of the side groups.

The simple analysis of the data presented in [18] and outlined here reveals that all the molecular weight dependence of the anomalous T_g reductions is contained in the slope parameter $\alpha(M_w)$. As discussed above, $\alpha(M_w)$ is not proportional to $M_w^{1/2}$, thus requiring another description of α on M_w. An empirical approach leads to Fig. 6 where the slope parameter is plotted as a function of $\log(M_w)$. The excellent agreement of the data with a straight line in this plot makes it possible to parameterize the data as

$$\alpha(M_w) = b\ln(M_w/M_w^*); \tag{4}$$

where $b = (0.70 \pm 0.02)$ K/nm and $M_w^* = (69 \pm 4) \times 10^3$. Without at least an intuitive reason for this functional form, this expression must be regarded as simply a convenient parameterization of the data and any expression that parameterizes the data accurately is equally valid. The extrapolation of the best fit line in Fig. 6 to $\alpha = 0$ results in $M_w^* = (69 \pm 4) \times 10^3$. This limit is illustrated by the dashed line labeled M_w^* in Fig. 5. M_w^* is obviously a lower limit for observing *any* effect due to the mechanism causing T_g reductions in thin films for any temperature up to T^*. A way to quantify the limiting M_w behavior in a way which is more directly comparable to experimental data, is to consider the smallest value of M_w for which T_g reductions can possibly be observed. The dashed line in Fig. 5 labeled by M_w^{**} results in no T_g reductions resulting from the thin film mechanism for *any* film. The slope of this line, $\alpha \sim 0.05$ K/Å, can be compared to Fig. 6 to obtain a lower limit $M_w^{**} \sim 150 \times 10^3$. In practice, the lower limit may be extended even further by making comparison to T_g reductions observed in the low M_w limit. Reductions in T_g for low M_w free-standing films (discussed in more detail below) have been attributed to a finite size effect due to an intrinsic length scale for co-operative dynamics [25]. For some values of M_w, these two mechanisms resulting in T_g reductions must both exist. We recall that in the high M_w regime, the bulk

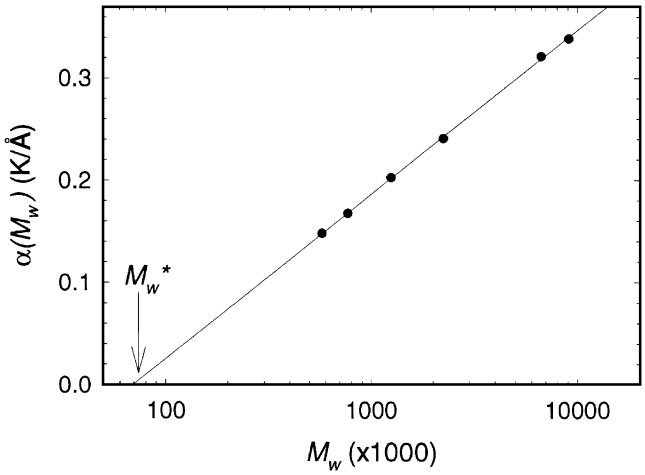

Fig. 6. Plot of the parameter representing the slope, α, of the reductions in T_g with h as a function of M_w.

mechanism and chain confinement mechanism compete, resulting in a sharp crossover determined by a switch of the most efficient mode for mobility. In an analogous way, the competition between chain confinement at high M_w and finite size effects at low M_w, must also be determined by the most efficient mechanism and result in a crossover of behavior. Reductions resulting from finite size effects, rather than chain confinement effects, are observed for free-standing films with thickness $h \lesssim 500$ Å. A fit to all the data in the low M_w regime where the finite size effects dominate, is indicated as the solid curve in Fig. 5. The estimated crossover M_w, is illustrated by the dashed line labeled M_w^{***} between (h^*, T_g^*) and tangent to the low M_w curve. From the slope of this line, $\alpha \sim 0.1$ K/Å, and Fig. 6 the crossover M_w can be estimated to be $M_w \sim 300 \times 10^3$. This is in excellent agreement with the study of the low M_w regime discussed in [25,36] and outlined below.

To summarize, the experimental data indicate four important results. (1) The sudden transition from bulk behavior to the linear reductions in T_g, indicate a competition between two distinct mechanisms. (2) Intersection of the best-fit lines to the reduced T_g values at (h^*, T_g^*) results in Eq. (3). (3) The slope parameter $\alpha(M_w)$ is given empirically by Eq. (4). (4) The crossover from the high M_w to low M_w regime is estimated to occur at $M_w \sim 300 \times 10^3$. Combining Eqs. (3) and (4) results in a simple expression for the T_g reductions in terms of film thickness and molecular weight dependence:

$$(T_g - T_g^*) = b\ln(M_w/M_w^*)(h - h^*). \tag{5}$$

Fig. 7 tests the scaling of this expression explicitly, and all the reduced T_g values for all thicknesses and molecular weights in the high M_w regime are very well

described by Eq. (5). Not only does this expression quantify the six M_w values studied with only four parameters, but all the T_g reductions due to confinement effects in general, are expected to be described by this expression as well.

4.1.1. Importance of annealing history

A concern associated with the sample preparation of high M_w polymer chains is the annealing history of the sample. In order to properly characterize the effects of chain confinement, we should study samples where the chains have been annealed to establish an equilibrium distribution of chain conformation. This is expected to require annealing times on the order of the reptation (or terminal) time τ_r. Measurements of the creep compliance of PS with $M_w = 385 \times 10^3$ reveal that the end of the 'plateau' region corresponding to the reptation time occurs at $\tau_r \sim 3 \times 10^3$ s at a temperature of 388 K [48] (the annealing temperature of the samples of the high M_w study). Since $\tau_r \sim M_w^{3.4}$, we can obtain τ_r for the various M_w values of this study to establish annealing times t. For the lowest two M_w values, 575×10^3 and 767×10^3, the relaxation times are $\tau_r \sim 3$ and 9 h, respectively, and the annealing time $t > \tau_r$. We would then conclude that these samples are sufficiently annealed. However, for higher molecular weights this is not true, and $t \ll \tau_r$. In particular, the longest chains of this study have $\tau_r \sim 4.5$ years. Clearly, this timescale is not easily accessible to experiment. Simply raising the annealing temperature is also not feasible since holes will form in the films. While hole formation is an indication that the polymers are mobile, this should *not* be taken as an indication that τ_r is on an experimental time frame. This is because hole

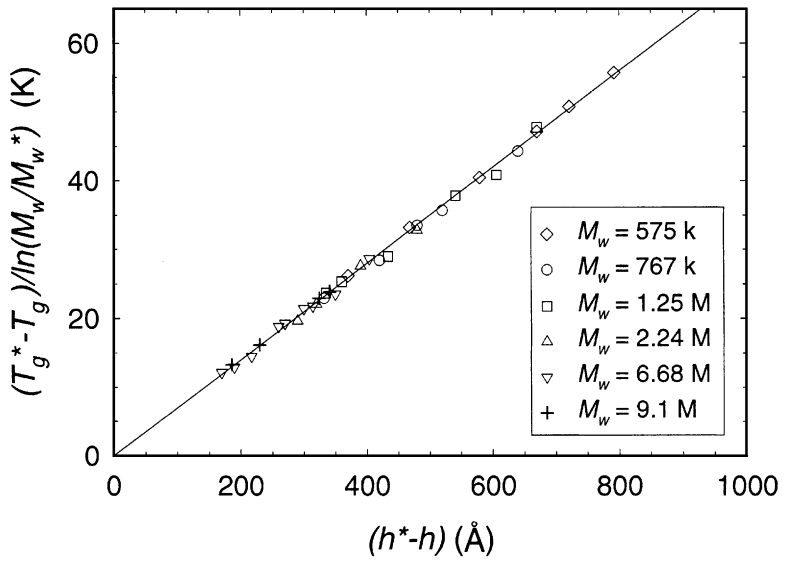

Fig. 7. The scaling behavior of the expression derived in the text, relating T_g in the high-M_w regime to both M_w and h.

growth is a result of surface tension, which provides a strong driving force to lower the free energy. This driving force may be large enough to result in alignment of the chains and resulting enhancement of the dynamics compared to τ_r. For example, a PS film with $h = 100$ nm, $M_w = 767 \times 10^3$ and at a temperature of 388 K, has been observed to exhibit a reduction in the viscosity of at least an order of magnitude, as a result of non-linear viscoelastic effects (shear-thinning) [49]. Annealing the highest M_w film would require raising the temperature to 433 K for 12 h, which would unfortunately result in a dewetted film. Given that there are some samples for which it is not feasible to anneal the samples for $t > \tau_r$, it is important to determine the effect of this on the measured T_g. We proceed by discussing several reasons why the annealing time is sufficient for the purposes of a T_g measurement.

The glass transition in the bulk is dependent on segmental mobility in the PS chains. As all the subchains of length less than the entanglement number N_e, can relax any non-equilibrium features of size $\sim R_{ee}\sqrt{N_e/N}$, where N is the number of monomers, equilibrium configurations at the length scale of segmental mobility are easily reached. This point is also made evident by the fact that while the reptation time in the bulk is strongly M_w-dependent, the glass transition for high M_w, polymers is not. Measurements of shear storage modulus for various M_w reveal this very clearly and relaxation of the rouse modes faster than those corresponding to N_e, are the relevant criteria for annealing. Studies of creep compliance show that for PS at $T = 388$ K, this criterion corresponds to a time $\tau_{N_e} \sim 100$ s [48]. For example, non-equilibrium density fluctuations can be relaxed without a re-ordering of the entanglement network. For this case, relaxations of the subchains ($\sim N_e$) combined with the associated expansion or compression of the entanglement network is all that is required. This means that all the chains are annealed for times $t > \tau_{N_e}$, sufficient for the measurement of the usual glass transition. While perturbations like density fluctuations are relaxed easily, any anomaly in the glass transition which is dependent on M_w and, hence, chain confinement effects, may still be influenced by annealing times $\tau_{N_e} < t < \tau_r$.

By definition, a chain-confinement effect has to depend on deviations from the bulk equilibrium conformation of the chains. While this means it is necessary to consider anisotropy in chain conformations due to spincoating or any other non-equilibrium process in the preparation of the samples, the anisotropy induced by sample preparation cannot have the strong film thickness dependence observed in our measurements. To illustrate this we consider the specific case of spincoating, although the argument is valid for any aspect of the sample preparation. During spincoating, a chain will be stretched in the radial direction as a result of the shear forces acting on it. This force, however, will be the same for any chain *regardless of the film thickness* and, as such, a film with thickness $h > h_0$ should exhibit the *same reductions* in the glass transition as a film with $h < h_0$. As this is not what is observed, the insufficient annealing time cannot explain our measurements. We reiterate that for a film with $M_w = 6.68 \times 10^6$ and $h \sim 1000$ Å, the measured value of T_g is in agreement with the literature value of the bulk T_g, while for a film

only 300 Å thinner, a reduction of ~ 50 K is observed. There are two additional reasons why the annealing history of the samples is sufficient for a reliable measure of chain confinement effect on the T_g value. The plot of α as a function of M_w (Fig. 6) does not illustrate any change in the behavior for chains that are annealed for $t > \tau_r$ ($M_w = 575 \times 10^3$, 767×10^3) and chains for which $t < \tau_r$ ($M_w = 1250 \times 10^3$ up to 9100×10^3). Finally, the dependence of the slope parameter α on M_w becomes weaker with increasing M_w. This dependence is inconsistent with the interpretation that the annealing history is responsible for the observed data. If non-equilibrium effects were an important contributing factor to the observed T_g reductions then the films with $t \ll \tau_r$ (i.e those with the highest M_w) would exhibit the largest deviations from equilibrium chain configuration and, thus, would show the largest dependence of T_g anomalies with M_w.

4.2. T_g for free-standing films with $M_w \leq 378 \times 10^3$

For PS molecules with $M_w \leq 378 \times 10^3$, the behavior is markedly different than that for the high M_w. The M_w dependence, which is such a strong distinguishing feature of the high M_w data, is either much weaker or vanishes entirely for the low M_w PS free-standing films. This is made explicitly clear in Fig. 5, where the M_w dependence observed for high M_w polymers, is extrapolated to polymers with $M_w = 150 \times 10^3$ and 300×10^3. The comparison of these extrapolations with the solid curve representing the low M_w data ($100 \times 10^4 \lesssim M_w \lesssim 400 \times 10^3$) shows explicitly the extreme deviations from the measured T_g values. In addition, the film thickness dependence of the measured T_g values is qualitatively different for the low M_w polymers. The linear function, which is so successful in describing the high M_w data, provides a poor description of the low M_w data. In fact, except for the magnitude of the effect, $T_g(h)$ seems more similar to that of the supported PS films. This comparison extends far enough that we can use Eq. (2), the relation used to describe supported PS and PMMA data, to describe the T_g data for the low M_w free-standing films. If we fix the power $\delta = 1.8$ as was used for supported PS films, then we obtain a best-fit to the data for a length scale $a = 78$ Å. The fact that the length scale for free-standing polymer films is twice that found for supported films, suggests that the mechanism that decreases T_g in the two different types of sample, is identical. This correspondence also reveals the importance of the free surface in causing the effect. For instance if there is a region of thickness ξ, near the free surface which decreases T_g, then in a free-standing film $\Delta T_g \sim 2\xi/h$, but in a supported film $\Delta T_g \sim \xi/h$, because the substrate eliminates the other free surface. The result of this is that for an effect caused by anomalous properties of a near free surface layer, we expect that a supported film of thickness h, will be identical in behavior to a free-standing film of thickness $2h$. As first noted in references [25,36], this direct correspondence is exactly the behavior observed between supported PS films and free-standing PS films with $M_w \leq 378 \times 10^3$. We note that the lack of M_w dependence suggests that chain confinement, which is so obviously dominant in films of higher M_w polymer, is not a large contributing factor to the effects observed in the lower M_w free-standing films or

in supported polymer films. The correspondence between the data for free-standing and supported films also shows that the effects of the substrate in the experiments of reference [16] are not significant. Such agreement between two different sample geometries, emphasizes the validity of the results and provides strong motivation for a shift of emphasis from quantifying to explaining T_g anomalies in thin polymer films.

5. Models used to describe T_g data

Perhaps the simplest explanation for reduced T_g values in thin films is a reduced average value of the density. For both supported [50] and free-standing films [26], measurements aimed at testing this idea have been performed and have revealed no anomalies in the density. For the case of the free-standing films, the magnitude of the T_g reductions coupled with the sensitivity of the density measurements, were such that if the T_g reductions were simply due to reduced density, then these density anomalies would have been observed. A number of recent publications have put forth ideas aimed at explaining the origins of the T_g reductions observed in thin free-standing films of PS. Like the suggestion provided by the data in Fig. 4, most of these models deal with either the high M_w or low M_w data. One proposed explanation has been suggested by Ngai on the basis of his coupling model to glass transition dynamics [51,52]. This approach is the only one that has attempted to couple conventional ideas of glass transition dynamics with polymer chain confinement. For a detailed discussion of these ideas the reader should consult references [51,52]. A second model that has been proposed to explain T_g reductions in thin films, is that of Jiang et al. [53]. This model attempts to explain anomalous dynamics in many confined systems. For polymer films, the model predicts *no dependence* of T_g reductions on the M_w value and $T_g(h) \sim 1/h$. The model is said to compare favorably with the free-standing film data of reference [23], even though the observed $T_g(h)$ is far from the model behavior and available experimental results [24] did, in fact, show a strong M_w dependence.

A recent model introduced to explain the data for the low M_w free-standing films (or supported films), is the model of Long and Lequeux [54,55]. This model is based on the idea that thermally-induced density fluctuations are the dominant factor in determining the glass transition in bulk or thin films. The formation of the glassy state upon cooling the liquid is described as a rigidity percolation [56]. The anomalous behavior of T_g in thin films is described as a transition from a 3-dimensional to a 2-dimensional (in the plane of the film) rigidity percolation. The idea behind the model is intuitively pleasing and it also leads to many aspects of bulk glass transition behavior in the existence of finite size effects. Furthermore, the model does not require introduction of any fitting parameters to give qualitative agreement with both bulk and thin film behavior. There are, however, a number of issues, that warrant further consideration. First of all, it is not clear that the ideas used to describe the bulk glass transition, are consistent with most experimental data, a problem previously faced by other free volume percolation

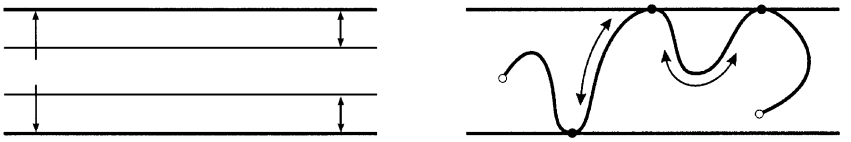

Fig. 8. (a) Illustration of the parameters relevant to the model dealing with supported films and the free-standing films in the low-M_w regime discussed in detail in the text. (b) The 'sliding' mode proposed in the model by de Gennes to explain the free-standing film results in the high-M_w regime.

models [57]. For the specific case of thin films, there are additional issues, which need to be considered. For instance the model predicts the parameter δ in Eq. (2) to be universally 1.5, irrespective of the polymer. While this agrees with $\delta = 1.8$ for PS, it is much different than $\delta = 0.8$ for PMMA [20]. Finally, the model describes the glass transition as a percolation of rigid clusters in the plane of the film, averaging over the heterogeneous dynamics in the direction normal to the film. The result of this procedure is that while the model can describe, approximately, the $1/h^{\delta}$ behavior observed for PS films, it is not as easy to explain the important experimental fact that a free-standing film of thickness h has a T_g reduction, which is quantitatively very similar to a supported film of thickness $h/2$. As explained above, this comes naturally from an explicit consideration of the effect of the free surface.

5.1. Layer model with dynamic heterogeneities

A model has been developed to describe the T_g in the low M_w free-standing films based on the idea of a characteristic length scale for dynamics in glass forming materials [25]. The model describes the film as fundamentally inhomogeneous with a layer near each free surface that has faster dynamics. These faster dynamics are simply modeled by introducing a different T_g near the surface, denoted T_g^{surf}. It is further argued that the size of this surface region should be essentially the same as the temperature-dependent length scale for glass transition dynamics, $\xi(T)$. This leads to a picture of free-standing films such as that shown in Fig. 8a. Following evidence from simulations and experiments, the average glass transition for a film of thickness h, is considered to be the relevant quantity for comparison with experimental data and is simply calculated to be

$$T_g(h) = T_g^{\mathrm{bulk}} - \frac{2\xi(T_g)\left(T_g^{\mathrm{bulk}} - T_g^{\mathrm{surf}}\right)}{h}. \tag{6}$$

In order to fit the experimental data, a parameterization for $\xi(T)$ has to be introduced. Following the original idea of Adam and Gibbs [5], as well as the recent simulations of glass forming liquids [7–9], a parameterization which allows $\xi(T)$ to increase with decreasing temperature is chosen. In general, we may write $\xi(T) = \xi(T^{\mathrm{ref}}) + \sigma(T - T^{\mathrm{ref}})^{\gamma}$. The remaining step in choosing the parameteriza-

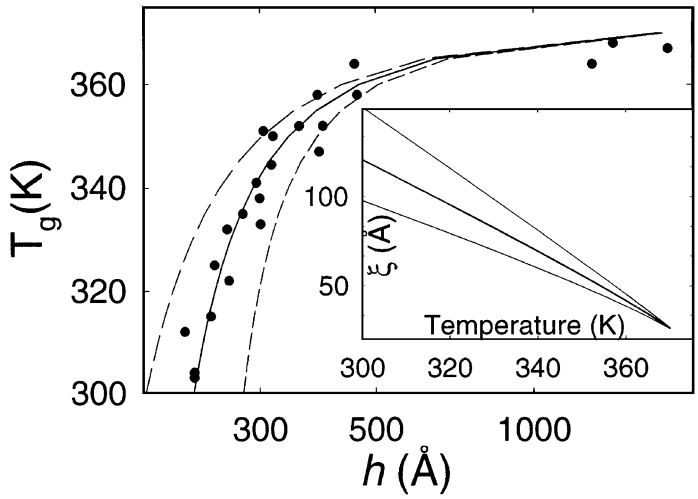

Fig. 9. T_g in free-standing films vs. h for the low-M_w regime. The solid line is the best fit to the data with the model described in the text. The inset is a plot of the size of the surface region with enhanced mobility as determined by the fits of the model to the data.

tion is to simply specify the reference temperature T^{ref}. There are two natural choices for T^{ref}. Since the data may only be used to describe $\xi(T)$ for $T < T_g^{\mathrm{bulk}}$, the bulk value of T_g is one natural choice. Alternatively, since the $\xi(T)$ is strongly linked with the length scale for co-operative dynamics, the temperature below which co-operative dynamics becomes important, T^{ons}, is another natural choice. Since independent estimates for T^{ons} and $\xi(T^{\mathrm{ons}})$ exist, this second parameterization allows us to have only three undetermined parameters. While this is more than the two parameters of Eq. (2), the advantage of the approach is that the parameters have a well-defined physical origin, which may be compared with other approaches. Furthermore, the value of T_g^{surf} may also be compared with independent estimates as may $\xi(T_g)$. In using either parameterization for $\xi(T)$, the best fit T_g^{surf} was found to be 305 ± 5 K, and the *actual values* of $\xi(T)$ were found to be the same within the fitting uncertainties for both parameterizations. A detailed discussion of the fitting is given in reference [36]. We note that this model with the same parameters, is also able to quantitatively describe the results for supported PS films as well as the very interesting behavior observed for grafted PS films [25].

5.1.1. Possible implications for the length scale of glass transition dynamics

Fig. 9 shows the T_g data for the low M_w, free-standing films, with an inset showing the values of $\xi(T)$, which produce the fit. Also shown is an estimate of the range of $\xi(T)$, and the resulting effect on the calculated T_g values. The solid line is the curve $\xi(T_g) = 22$ Å, $\sigma = 2.1$ and $\gamma = 0.90$; but as noted in reference [25] for values of h where T_g reductions are observed, very similar values of $\xi(T)$ are found using the parameterization for $T^{\mathrm{ref}} = T^{\mathrm{ons}}$, and the curve is then described by the

parameters $T^{ons} = (485 \pm 6)$ K, $\gamma = 2.00 \pm 0.1$, and $\sigma = (2.95 \pm 0.3) \times 10^{-3}$. The $\xi(T)$ presented in the inset is the most remarkable aspect of this particular approach. In addition to providing a description of T_g reductions in thin polymer films within a context which is the same used to describe finite size effects in other sample types, it also provides the first prediction of the length scale for the dynamics over an extended temperature range below the bulk T_g. While the indirect nature of the approach means we cannot be sure it is a correct description, the implications of the predicted $\xi(T)$ may be crucial to developing a fundamental understanding of dynamics in glass forming materials. The most notable aspect of the $\xi(T)$ is that the values *do not diverge* at the Vogel–Fulcher temperature, T_0. This fact follows trivially from the measurements of $T_g < T_0^{bulk}$. While finite $\xi(T)$ for all temperatures (at least as low as 300 K) seems a departure from some traditional ideas of the glass transition, it is a perfectly natural picture. Within the context of co-operative motion, we can express the relaxation time in the material as $\tau(T) \propto \exp[N(T)\varepsilon^*/T]$ where $N(T)$ is the average number of monomer units making a co-operative rearrangement, and ε^* is related to a monomeric activation barrier for rearrangement. In order to relate this to $\xi(T)$, we need to introduce a relation between $N(T)$ and $\xi(T)$. The most common approach is to assume a roughly spherical region within which *all* particles take part in a structural rearrangement so that $N \sim \xi^3$. As a result of certain theoretical approaches [6] as well as many recent simulations, it is becoming increasingly obvious that such an approach is probably incorrect. Co-operative motion does not have to involve all molecules or segments within a volume $\sim \xi^3$, and instead, the evidence suggests that the collective motion occurs in string-like loops so that $N \sim \xi$. We can use the data for $\xi(T)$ to estimate characteristic relaxation times. We ignore the explicit temperature dependence in $\tau(T)$, which is negligible compared to the strong effect of $\xi(T)$. Since we know that ξ varies from the nearest adjacent spacing ($\xi_0 \sim 5$ Å) at high temperatures where $\tau = \tau_0 \sim 10^{-12}$ s to ~ 25 Å at T_g [58] where $\tau \sim 10^2$ s, we can write $\tau(T) = \tau_0 \exp[(\xi(T) - \xi_0)\varepsilon]$ where $\varepsilon \simeq 1.6$ based on the above limiting values. If we use this relation and the data in the inset of Fig. 9, then we calculate that at a temperature of 360 K (10 K below T_g bulk $\xi \sim 50$ Å), $\tau \simeq 10^{12}$ years. Thus, we see that even for values of $\xi(T)$ which are still truly microscopic (i.e. not diverging as often assumed), the relaxation times rapidly become larger than any experimentally accessible time. This analysis also suggests that for the case of PS, if we imagine that it is only possible to measure relaxation times as large as, for example, 1 year, then finite size effects will only be observed for samples confined to dimension of ≤ 30 Å. While divergence of $\xi(T)$ may be a theoretically appealing picture, it is obviously *not required* to explain the very long relaxation time for $T < T_g$ and, in fact, very reasonable values come from the length scale $\xi(T)$ in Fig. 9. The temperature dependence of the relaxation times is now determined by the temperature dependence of ξ. With this in mind, we consider the fluctuation theory of Donth [59,60]. In this theory Donth derives the relation $N \sim (T^{ons} - T)^2$, to describe heat capacity and dielectric data at temperatures above T_g, but below T^{ons}. For comparison, we recall that in fitting the T_g

data, we could parameterize $\xi(T)$ in terms of T^{ons}. For that case, we were able to describe the data for $\xi(T) \simeq (T^{\text{ons}} - T)^2$, which for $\xi \sim N$ means $N \sim (T^{\text{ons}} - T)^2$. This coincidence of temperature dependence might suggest that a uniform approach to describing dynamics at temperature over a large range encompassing the T_g value, may be possible.

5.2. The sliding model of de Gennes for high M_w free-standing films

Recently de Gennes has proposed a model that explains many of the qualitative features of the T_g reductions in free-standing films in the high M_w regime [47]. As suggested by the data, a competition between two different modes of mobility is proposed: the usual small length scale segmental mobility associated with the bulk glass transition; and a second mode where the polymer chain 'slides' along the direction of the primitive path. This 'sliding' motion is further shown to be important only in thin films. As the film thickness is decreased below $h \sim R_{EE}$, most chains will have contacts with the free interface as illustrated in Fig. 8b. There are two types of segments, loops [AB′] and bridges [AB], which are free to slide. The sliding motion is only hindered by side chains as the motion at the ends of the segments are unrestricted due to the existence of a highly mobile surface layer. In the bulk, the sliding motion is inhibited because the chain ends would have to invade new territory with a large associated activation barrier, making the usual co-operative motion a more efficient mechanism. The model proposed by de Gennes incorporates this sliding mechanism and the competition between the two modes. At high M_w, the model predicts a *linear* dependence of T_g on the film thickness h as observed in the data. The model also predicts a limiting M_w, beyond which the h dependence of T_g saturates. At present, though there is qualitative agreement with the data, quantitative differences still exist and the model does not yet explain the M_w dependence and the convergence of the extrapolated data at the point (h^*, T_g^*).

There are more rigorous experiments that may test the validity of the model. Reductions in T_g may be reduced or suppressed in branched or comb polymers since the branches would increase the activation barrier associated with sliding. Another test of the model might be revealed by studying the chain end dynamics of chains in a free-standing film. In the case of the chain segments terminated by the chain ends, as shown by [BC] in Fig. 8b, sliding is blocked as it is in the bulk because the end will not invade new territory due to the relatively large activation barrier. However, the sliding should only be surpressed for a slide away from the free surface; conversely, a slide towards the surface is very favorable since this creates large amounts of free volume within the film. In effect, this process will drive the chain end towards the free surface where the end may be trapped based on entropy arguments [29]. Generally, it is assumed that a random diffusive process is responsible for getting chain ends towards the free surface. However, given the sliding mechanism, the dynamics of chain ends migrating to the interface should be much faster since the chain end is 'driven' towards the surface.

6. Future issues

It is evident now that there is certainly an experimental consensus about film thickness dependence of the T_g in thin polymer films. While there are no contradictions persisting in the literature, there are some differences between different studies which, though still consistent, could be misconstrued as contradictory. The most current of these concerns the idea of the breadth of the glass transition in thin films. It is an intuitive idea that the dynamics in a very thin film will be strongly heterogeneous with higher mobility near the free surface than in the interior of the film. This heterogeneity in the dynamics would be expected to manifest itself in two different ways. In the first case, direct measurements of the relaxation should show a broadening, which increases as the film thickness is lowered. Additionally, we might reasonably expect to observe a broadening of the glass transition as different parts of the film undergo the glass transition at different temperatures. Again, this broadening should be more pronounced in thinner films. For supported PS films, such a broadening of the glass transition has recently been observed and studied [17]. For free-standing films, however, the situation is different and despite detailed analysis [18,36], such a broadening is not observed. This lack of broadening does not necessarily disagree with the observations for supported films. In all of these studies, the T_g is measured by the change in the expansivity, and it is not necessarily clear that the coupling between the expansivity and the dynamics is the same for the case of unconstrained free-standing films and laterally constrained supported films.

It is probably more fruitful to directly measure relaxation behavior in order to consider this issue of broadening. Reports of such measurements have recently begun to appear but, as we shall see, the results are not yet entirely convincing. The first measurements of relaxation in thin films were dynamic light scattering measurements on free-standing films [39]. The temperature-dependent relaxation times in these studies were entirely consistent with T_g measurements of similar samples. The shape of the relaxation function, however, was found to be the same as that for bulk polymer, though it should be noted that due to the difficulty of the experiments, the signal-to-noise ratio did not allow a high precision for the stretching parameter β. This same study also considered adhesion measurements on supported films and collectively found that the relaxation behavior was well described by using a Vogel–Fulcher form with a shift in T_0 equal in magnitude to the observed shift in T_g. The implication of this was that the fragility index (T_g/T_0) in the free-standing films is greater than that in the bulk. For the case of PS films between metallic electrodes, Fukao and Miyamoto have recently presented an exhaustive study of dielectric relaxation behavior. They observe a distinct broadening of the relaxation function for thin films as expected. A complication of this interpretation is that the films were subject to evaporation of a metallic electrode, which can plasticize the film to produce these same results. Overall, it is clear that future efforts should be concentrated on direct measurements of relaxation behavior for the case of both free-standing and supported polymer films.

A final area of study, which could help to further develop our understanding of

T_g reductions in thin polymer films concerns the crossover from the qualitatively different behaviors observed between low M_w and high M_w PS films. For the values of M_w that have been studied, the crossover appears to be very sharp and there are no values of M_w for which an intermediate behavior has been observed. It is possible, however, that a detailed study of films with $378 \times 10^3 < M_w < 575 \times 10^3$ will show such behavior and allow us to learn more about the relative effect of the two competing mechanisms.

7. Conclusions

Studying the glass transition of confined glass forming systems is a promising technique to investigate the existence of a characteristic length for glass transition dynamics, and to examine the effect of confinement on polymer dynamics. Since the original report of anomalies in the T_g value of thin polymer films, there has been increasing interest in such measurements. For polystyrene films supported on substrates, a large number of studies have been performed, and a clear experimental consensus is evident. In addition to the anomalies in the T_g value, systematic trends have also been observed in the thermal expansion of both supported and free-standing films. Despite qualitative agreement between a large number of different studies, scatter in the data attributable to differences in the substrate, has prevented serious attempts at modeling the behavior. Measurements of free-standing films have not only circumvented this difficulty, but have also led to observation of the polymeric phenomenon of chain confinement that had not been shown to similarly affect the dynamics of the supported films. This has led to a very complicated dependence of the film thickness-dependent T_g values in free-standing films. Since the first report of T_g measurements in free-standing films, a number of models have been introduced in an attempt to explain the results. We have discussed in detail two such models; one related to chain confinement and one related to a characteristic length scale for dynamics in the glass forming material.

Acknowledgements

We gratefully acknowledge discussions with P.G. de Gennes, J.R. Dutcher, R.A.L. Jones, J. Mattsson and G.B. McKenna. Financial support from EPSRC of the UK and NSERC of Canada is gratefully acknowledged.

References

[1] M.H. Cohen, D. Turnbull, J. Chem. Phys. 31 (1959) 1164.
[2] W. Götze, L. Sjögren, Rep. Prog. Phys. 55 (1992) 241.
[3] J.H. Gibbs, E.A. DiMarzio, J. Chem. Phys. 28 (1958) 373.
[4] E.A. DiMarzio, A.J.M. Yang, J. Res. N.I.S.T. 102 (1997) 135.

[5] G. Adam, J. Gibbs, J. Chem. Phys. 43 (1965) 139.
[6] S. Edwards, T. Vilgis, Physica Scripta T13 (1986) 7.
[7] C. Donati, S. Glotzer, P.H. Poole, W. Kob, S.J. Plimpton, Phys. Rev. E. 60 (1999) 3107.
[8] W. Kob, C. Donati, S.J. Plimpton, P.H. Poole, S.C. Glotzer, Phys. Rev. Lett. 79 (1997) 2827.
[9] C. Bennemann, C. Donati, J. Baschnagel, S. Glotzer, Nature 399 (1999) 246.
[10] K.F. Mansfield, D.N. Theodorou, Macromolecules 24 (1991) 6283.
[11] C.L. Jackson, G.B. McKenna, J. Non-Cryst. Solids 221 (1991) 131.
[12] M. Arndt, R. Stannarius, H. Groothues, E. Hempel, F. Kremer, Phys. Rev. Lett. 79 (1997) 2077.
[13] R. Stannarius, F. Kremer, M. Arndt, Phys. Rev. Lett. 75 (1995) 4698.
[14] R.A.L. Jones, R.W. Richards, Polymers at Surfaces and Interfaces, Cambridge University Press, Cambridge, UK, 1999.
[15] R.M.A. Azzam, N.M. Bashara, Ellipsometry and Polarized Light, North Holland Publishing Company, Amsterdam, 1977.
[16] J.L. Keddie, R.A.L. Jones, R.A. Cory, Europhys. Lett. 27 (1994) 59.
[17] S. Kinawa, R.A.L. Jones, Phys. Rev. E63 (2001) 021501.
[18] K. Dalnoki-Veress, J.A. Forrest, C. Murray, C. Gigault, J.R. Dutcher, Phys. Rev. E 63 (2001) 031801.
[19] G.B. DeMaggio, W.E. Frieze, D.W. Gidley, M. Zhu, H.A. Hristov, A.F. Yee, Phys. Rev. Lett. 78 (1997) 1524.
[20] O. Prucker, S. Christian, H. Block, J. Rühe, C.W. Frank, W. Knoll, Macromol. Chem. Phys. 199 (1998) 1435.
[21] K. Fukao, Y. Miyamoto, Phys. Rev. E. 61 (2000) 1743.
[22] K. Fukao, Y. Miyamoto, Europhys. Lett. 46 (1999) 649.
[23] J.A. Forrest, K. Dalnoki-Veress, J.R. Stevens, J.R. Dutcher, Phys. Rev. Lett 77 (2002) 1996.
[24] J.A. Forrest, K. Dalnoki-Veress, J.R. Dutcher, Phys. Rev. E 56 (1997) 5705.
[25] J.A. Forrest, J. Mattsson, Phys. Rev. E 61 (2000) 53.
[26] J.A. Forrest, K. Dalnoki-Veress, J. Dutcher, Phys. Rev. E 58 (1998) 6109.
[27] J.R. Dutcher, K. Dalnoki-Veress, J.A. Forrest, in: S. Mann, G.G. Warr (Eds.), ACS Symposium Series 736, American Chemical Society, 1999.
[28] J.H. Kim, J. Jang, W.C. Zin, Langmuir 16 (2000) 4064.
[29] T.P. Russell, Communication.
[30] J.A. Forrest, R.A.L. Jones, The glass transition and relaxation dynamics in thin polymer films, in: A. Karim, S. Kumar (Eds.), Polymer Surfaces Interfaces and Thin Films, World Scientific, Singapore, 2000.
[31] J.L. Keddie, R.A.L. Jones, J. Isr. Chem. Soc. 35 (1995) 21.
[32] J.H. van Zanten, W.E. Wallace, W. Wu, Phys. Rev. E 53 (1996) R2053.
[33] J.L. Keddie, R.A.L. Jones, R.A. Cory, Faraday Discuss. 98 (1994) 219.
[34] Y. Grohens, M. Brogly, C. Labbe, M.O. David, J. Schultz, Langmuir 14 (1998) 2929.
[35] W.E. Wallace, J.H. van Zanten, W. Wu, Phys. Rev. E 52 (1995) R3329.
[36] J. Mattsson, J.A. Forrest, L. Börgesson. Phys. Rev. E 62 (2000) 5187.
[37] B. Frank, A.P. Gast, T.P. Russell, H.R. Brown, C. Hawker, Macromolecules 29 (1996) 6531.
[38] X. Zheng, M.H. Rafailovich, J. Sokolov et al., Phys. Rev. Lett. 79 (1997) 241.
[39] J.A. Forrest, C. Svanberg, K. Révész, M. Rodahl, L.M. Torell, B. Kasemo, Phys. Rev. E 58 (1998) R1226.
[40] D.B. Hall, J.C. Hooker, J.M. Torkelson, Macromolecules 30 (1997) 667.
[41] A.D. Schwab, D.M.G. Agra, J.H. Kim, S. Kumar, A. Dhinojwala, Macromolecules 33 (2000) 4903.
[42] Y.C. Jean, R. Zhang, H. Cao et al., Phys. Rev. B 56 (1997) R8459.
[43] L. Xie, G.B. DeMaggio, W.E. Frieze, D.W. Gidley, H.A. Hristov, A.F. Yee, Phys. Rev. Lett. 74 (1995) 4947.
[44] Y. Liu, T.P. Russell, M.G. Samant et al., Macromolecules 30 (1997) 7768.
[45] J. Hammerschmidt, W. Gladfelter, G. Haugstad, Macromolecules 32 (1999) 3360.
[46] K. Dalnoki-Veress, J.A. Forrest, P.-G. de Gennes, J.R. Dutcher. J. Phys. IV, 10 Pr7–221 (2000).
[47] P.-G. de Gennes, Eur. Phys. J. E2 (2000) 201.

[48] G. Strobl, The Physics of Polymers: Concepts for Understanding their Structure Behaviour, Second Edition, Springer-Verlag, Berlin, 1997.
[49] K. Dalnoki-Veress, B.G. Nickel, C.B. Roth, J.R. Dutcher, Phys. Rev. E 59 (1999) 2153.
[50] W.E. Wallace, N.C. Beck Tan, W.L. Wu, J. Chem. Phys. 108 (1998) 3798.
[51] K.L. Ngai, A.K. Rizos, D.J. Plazek, J. Non-Cryst. Solids 235–237 (1998) 435.
[52] K.L. Ngai, J. Phys. IV 10 Pr7–221 (2000).
[53] Q. Jiang, H.X. Shi, J.C. Li, Thin Solid Films 354 (1999) 283.
[54] D. Long, F. Lequeux, submitted to Europhys. Lett.
[55] D. Long, F. Lequeux, submitted to Euro. J. Phys. E.
[56] C. Moukarzel, P.M. Duxbury, Phys. Rev. E 59 (1999) 2614.
[57] M.H. Cohen, G.S. Grest, Phys. Rev. B 20 (1979) 1077.
[58] S. Kahle, J. Korus, E. Hempel et al., Macromolecules 30 (1997) 7214.
[59] E. Donth, S. Kahle, J. Korus, M. Beiner, J. Phys. I France 7 (1997) 581.
[60] H. Huth, M. Beiner, E. Donth, Phys. Rev. B 61 (2000) 15092.